JOURNAL OF SOLID STATE CHEMISTRY 69, 360–368 (1987)

Identifying Characteristics of the Fibrous Cesium Titanate $Cs_2Ti_5O_{11}$

L. A. BURSILL,*,[1] DAVID J. SMITH†,‡ AND JADWIGA KWIATKOWSKA*,§

*School of Physics, University of Melbourne, Parkville, 3052 Victoria, Australia; †High Resolution Electron Microscope, Department of Metallurgy and Materials Science, University of Cambridge, Pembroke Street, Cambridge CB2 3QZ, England; ‡Centre for Solid State Science and Department of Physics, Arizona State University, Tempe, Arizona 85287; §Institute of Nuclear Physics, radzikowskiego 152, 31-342 Krakow, Poland

Received July 14, 1986; in revised form December 23, 1986

Electron microscopic studies of the fibrous cesium titanate $Cs_2Ti_5O_{11}$ reveal characteristic features not readily apparent using standard methods of phase analysis (optical microscopy, X-ray diffraction). Its fibrous needle-like laths give characteristic diffuse scattering, complicating the indexing of electron diffraction patterns. The hydrated form $Cs_2Ti_5O_{11} \cdot (1 + x)H_2O$ ($0.5 < x < 1$) is typically grossly distorted, resembling pyrolytic graphite. $Cs_2Ti_5O_{11}$ is unstable when stored under ambient conditions at room temperature for ~1 year when disproportionation into $Cs_2Ti_4O_9$ and $Cs_2Ti_6O_{11} \cdot nH_2O$ occurs. The structure of $Cs_2Ti_5O_{11}$ and intergrowth defects in the unstable forms have been studied by high-resolution electron microscopy. It is evident that these phases would be undesirable in titanate ceramics such as SYNROC, which are designed for immobilization of radioactive $^{137}C_s$.

Introduction

The cesium titanate phase $Cs_2Ti_5O_{11} \cdot (1 + x)H_2O$, and its corresponding dehydrated form $Cs_2Ti_5O_{11}$, may occur as undesirable disequilibrium phases in some synthetic titanate ceramics designed for the disposal of radioactive ^{137}Cs (*1–3*). These phases were not readily detected as a minor component in SYNROC preparations, when optical microscopy or X-ray powder diffraction methods were employed (*4*). However, single phase preparations exhibit a characteristic fibrous morphology and give distinctive images and electron diffraction patterns (*1*). The hydrated cesium titanate phase has also been prepared by uptake from cesium hydroxide solution using crystalline hydrous titanium dioxide fibers ($TiO_2 \cdot nH_2O$) as ion-absorbants (*5*). It was shown that, following addition of Al_2O_3 and TiO_2 and calcination at 1000°C, a cesium priderite phase $Cs_xAl_xTi_{8-x}O_{16}$ ($x = 1.6$) may be prepared (*5*).

The purpose of this paper is to describe the distinctive morphology and electron diffraction patterns of the cesium titanate $Cs_2Ti_5O_{11}$ and to relate these properties to the crystal structure which was determined recently (*2, 6*). Other observations relevant to the chemical and physical stability of this

[1] To whom correspondence should be addressed.

0022-4596/87 $3.00

phase, and its defect structure, are also presented.

Experimental

The crystal growth conditions have already been described (*1*). The present results were obtained from preparations having an initial stoichiometry of $Cs_2O \cdot 4TiO_2$, but which were subsequently found to crystallize predominantly as $Cs_2Ti_5O_{11}$ (*2*). Initially, specimens were prepared for electron microscopy by grinding ceramic fragments under chloroform or acetone and dispersing the particles on holey carbon support films. There were some discrepancies between early X-ray powder data and the reciprocal lattices observed by electron diffraction. This resulted in part from the occurrence of both hydrated and dehydrated forms and from special features of the reciprocal lattices (described below). A comparison was then made between dry-ground dehydrated particles, mounted directly on grids without solvent, and particles obtained from a slurry ground under water. Some specimens were reexamined after a period of 18 months storage in a Pelco grid box, with a close-fitting but not airtight lid. These showed some significant structural changes related, as shown below, to the hydroscopic nature of this material, and its thermodynamic instability.

The crystals typically exhibited a lath-like fibrous habit (Fig. 1) and thin edges were examined using (i) the high-tilt (±60°, ±45°) side-entry goniometer of a JEM-100CX instrument in Melbourne, which provided the essential diffraction data; (ii) the Cambridge University high-resolution electron microscope (spherical aberration coefficient Cs = 2.7 mm), which provided 500-kV (1.8 Å) images; and (iii) the JEM-200CX instrument in Arizona (spherical aberration coefficient Cs = 1.0 mm), which provided images having ~2.5 Å resolution (following the 18 months storage of the specimens). Due to the characteristic growth habit, it was not possible to obtain the [010] lath axis as the projection axis for imaging or electron diffraction. Attempts were made to obtain transverse sections by mounting the fibrous crystals in Spurr's resin and using an ultramicrotome to cut thin sections. This proved unsuccessful, since the knife invariably pulled away fibrous material rather than cutting cleanly across the lath axis (see Fig. 3 below).

FIG. 1. Low magnification image showing characteristic lath-like habit of $Cs_2Ti_5O_{11}$.

Results

(*a*) *Morphology*. Figure 1 shows the characteristic lath-like habit of dispersed particles. Needles varied in length from 0.1 to 10 μm depending on the crystallization procedures. Only the smaller laths were sufficiently thin for transmission electron microscopy. Oriented intergrowths and overgrowths parallel to [010] were common

(Fig. 1), indicating rapid growth along [010] with (100) and (001) as slowly growing faces. These often showed lamellar-type growth steps and ledges. In many crystals there were fractures and displacements of one part of a lath with respect to another. These defects may have occurred during grinding of the specimens under chloroform. Freshly prepared crystals showed no evidence for plastic deformation, i.e., dislocations did not occur, and no significant evidence for chemical inhomogeneities, such as intergrowth defects, were found.

Specimens which had been soaked in water prior to dispersal on holey carbon films showed remarkable paracrystallinity (Fig. 2), often resembling in appearance graphitized carbon or fibrous minerals such as clays or asbestos. Structural sheets were observed to be grotesquely folded and interleaved, without translational or orientational symmetries and with extremely indistinct diffraction patterns. Such material would not be readily detected by X-ray or neutron powder diffraction, or by optical microscopy, if it occurred at phase or grain boundaries in, for example, a SYNROC ceramic subjected to a wet environment.

FIG. 2. Paracrystalline character of $Cs_2Ti_5O_{11}$ after deposition from a slurry formed by grinding freshly prepared material in water.

Thorough dehydration of the crystalline preparations, just prior to dry-mounting on holey carbon support films, yielded sharper electron diffraction patterns, but the morphology did not differ significantly from that of specimens which had been dispersed in chloroform or acetone. Attempts to examine preparations which were supposedly hydrated, according to X-ray powder diffraction, were unrewarding and gave results identical to those of dehydrated specimens. This indicates that dehydration probably occurred rapidly in the electron microscope (10^{-7} Torr total pressure at the specimen), especially in the thin crystals selected for study.

Specimens which had been microtomed showed another distinctive morphology (Fig. 3). They contained heavily deformed laths which gave the appearance of being pulled away in bundles from the thin section of epoxy. These also gave very indistinct diffraction patterns and, despite extensive searches, useful [010] sections could not be found.

Specimens which were reexamined after 18 months storage showed, in addition to the usual lath-like crystals, many small (30–200 Å diameter) roughly circular platelet-shaped crystallites, both on the surface of laths and on the adjacent carbon support film (Fig. 4). The laths now often contained extended dislocation-like defects for [100] projections (Fig. 5) and intergrowth defects for [011] projections (Figs. 6a and 6b). The platelet crystals were sensitive to the electron beam. When the beam was focused for high-magnification observation, the platelets became fluid and had high mobility on the carbon film and they

FIG. 3. Fibrous texture, showing gross mechanical deformation of $Cs_2Ti_5O_{11}$ after embedding in resin and sectioning with an ultramicrotome.

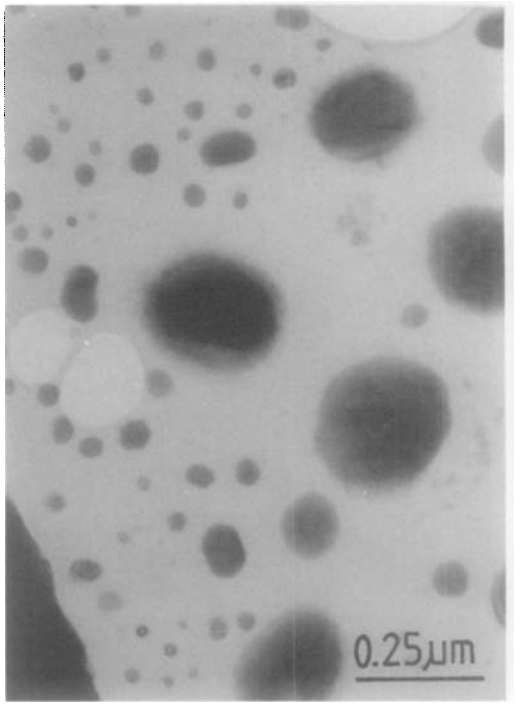

FIG. 4. Platelet crystallites which become mobile and eventually evaporate under a focused electron beam; note dimensions 30 Å $< D <$ 200 Å.

eventually disappeared, presumably by evaporation, so they may not survive a high radiation flux for very long.

(*b*) *Electron diffraction patterns*. Figure 7a shows the [001] projection of $Cs_2Ti_5O_{11}$ (a = 19.72 Å, b = 3.81 Å, c = 15.02 Å, β = 106.93°); SG : C2/m (*2*). Tilting by 16° about [100] to the [101] zone (Fig. 7b) shows one of the two most common and characteristic electron diffraction patterns. Note the intense continuous diffuse streaking parallel to [100] and the 75° angle between 010 and 111. Because of the distinctive appearance of this diffuse scattering, there was a tendency to record data for the [011] zone, rather than the principal [001] zone, which exhibits orthogonal axes and where the diffuse scattering almost disappears.

Precise [100] projections were quite difficult to obtain experimentally. Thus [110] (Fig. 8a) occurred frequently: note the 86.7° angle between 001 and 110. It was only

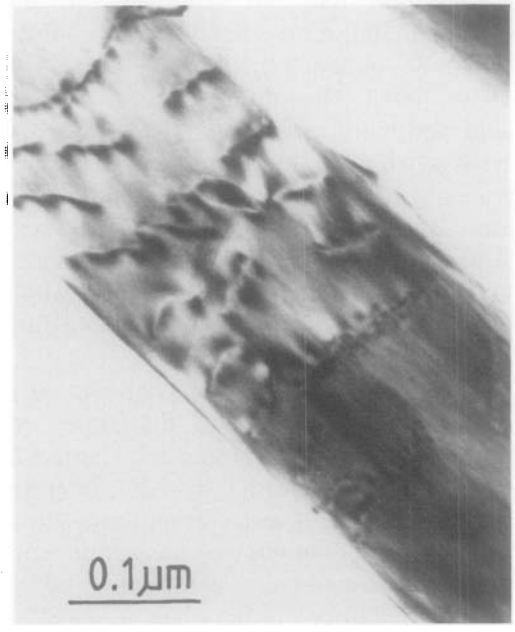

FIG. 5. Dislocation-type defects in a lath of $Cs_2Ti_5O_{11}$ after lengthy storage, [001] projection.

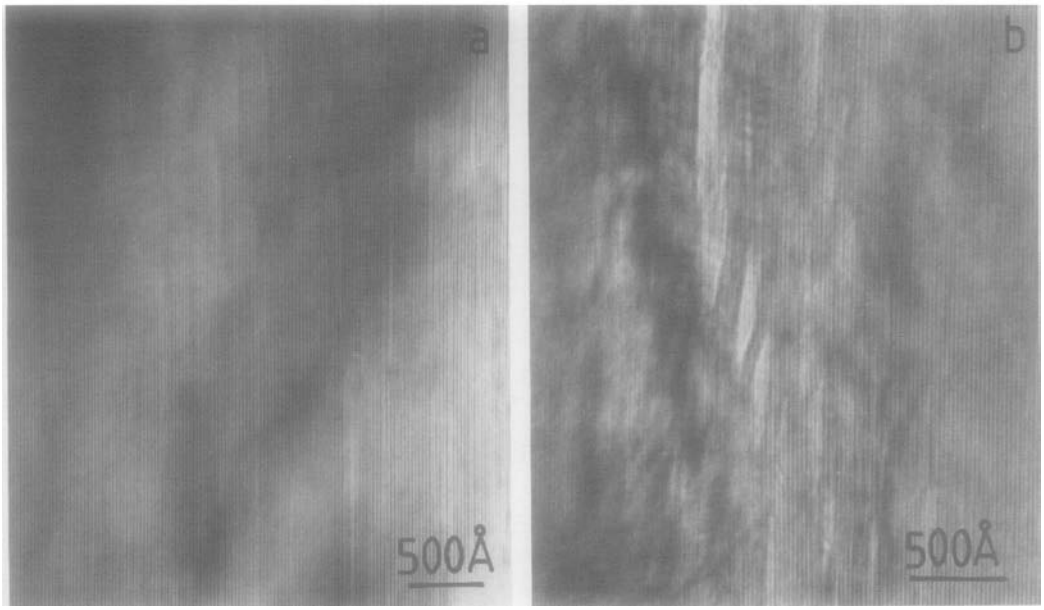

FIG. 6. Intergrowth defects in [100] projection of stored specimen. Note lamellae showing slightly larger fringe spacings than usual.

after the true monoclinic symmetry was established by X-ray precession photographs (*2*), that we searched for and obtained [100] reproducibly. This is shown in Fig. 8b, obtained by tilting 17° from [110] about [001]. This tilting experiment was achieved more readily at 500 kV when the relatively flat Ewald sphere allowed the two zones to be distinguished. Superstructures are also distinguishing features of these zones (Figs. 8a and 8b), with pronounced maxima on $(0, k + \frac{1}{2}, 0)$ reciprocal lattice planes, symmetrically placed with respect to the subcell.

The combined results for [100] and [001] explain the experimental difficulties referred to above concerning recognition of these zones. Thus tilting by ~20°, in either case, often gave a series of patterns showing virtually continuous changes in spot positions, resembling a deformation of the reciprocal lattice, rather than a series of distinct reciprocal lattice sections. Under these conditions, it was difficult to maintain the desired [010] tilt axes precisely in the plane of projection. Thus, much of the earlier diffraction data could not be indexed satisfactorily. Later, by first obtaining [001] or [100] exactly, as indicated by the orthogonal axes (Figs. 7a, 8b), and then maintaining [010] strictly, it became possible to obtain series of diffraction patterns consistent with the unit cell parameters obtained by X-ray methods (*2*, *6*). This was achieved more readily at 500 kV, and subsequently also at 100 kV, especially after the specimens had been carefully dehydrated prior to examination. (The presence of partially dehydrated crystals also contributed to the difficulty of indexing imprecisely oriented patterns.)

Further detailed studies have been made of the three-dimensional distribution of diffuse scattering which is a result of short-range ordering of Cs^{+1} cations in the structure (*7*).

The platelet-like crystallites (Fig. 4) gave diffraction patterns which indexed reason-

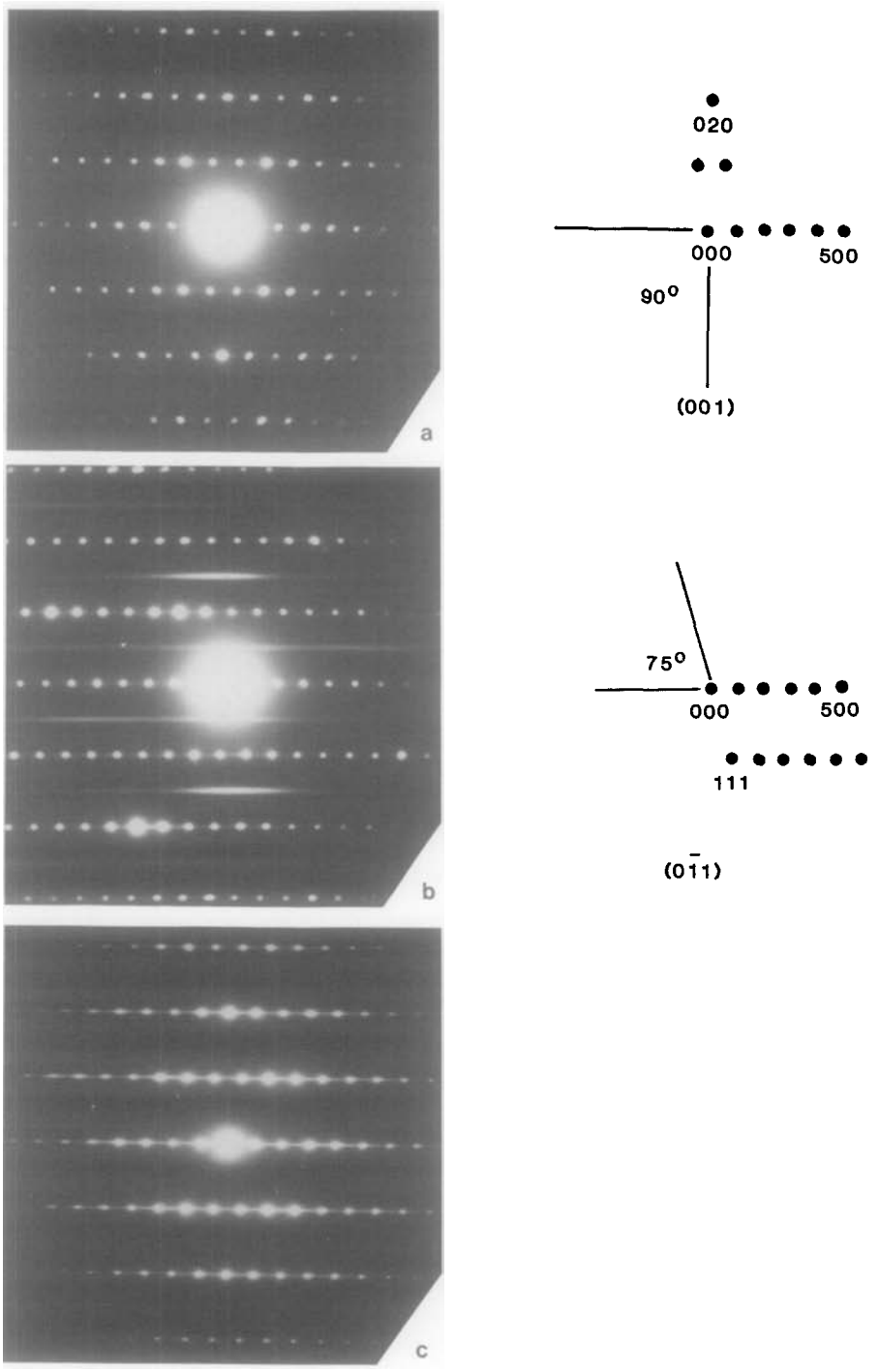

FIG. 7. (a) [001] and (b) [011] zone axis electron diffraction patterns of freshly prepared $Cs_2Ti_5O_{11}$. Note orthogonal axes in (a) and 75° angle between [010] and [111] in (b). Intense continuous diffuse streaking appears in (b) but is virtually extinguished in (a). The streaking is most intense *between* subcell rows, but it is also present through subcell spots, parallel to [100]. (c) [001] zone electron diffraction pattern of stored $Cs_2Ti_5O_{11}$. Note intense diffuse streaking along [100] passing through sharp spots.

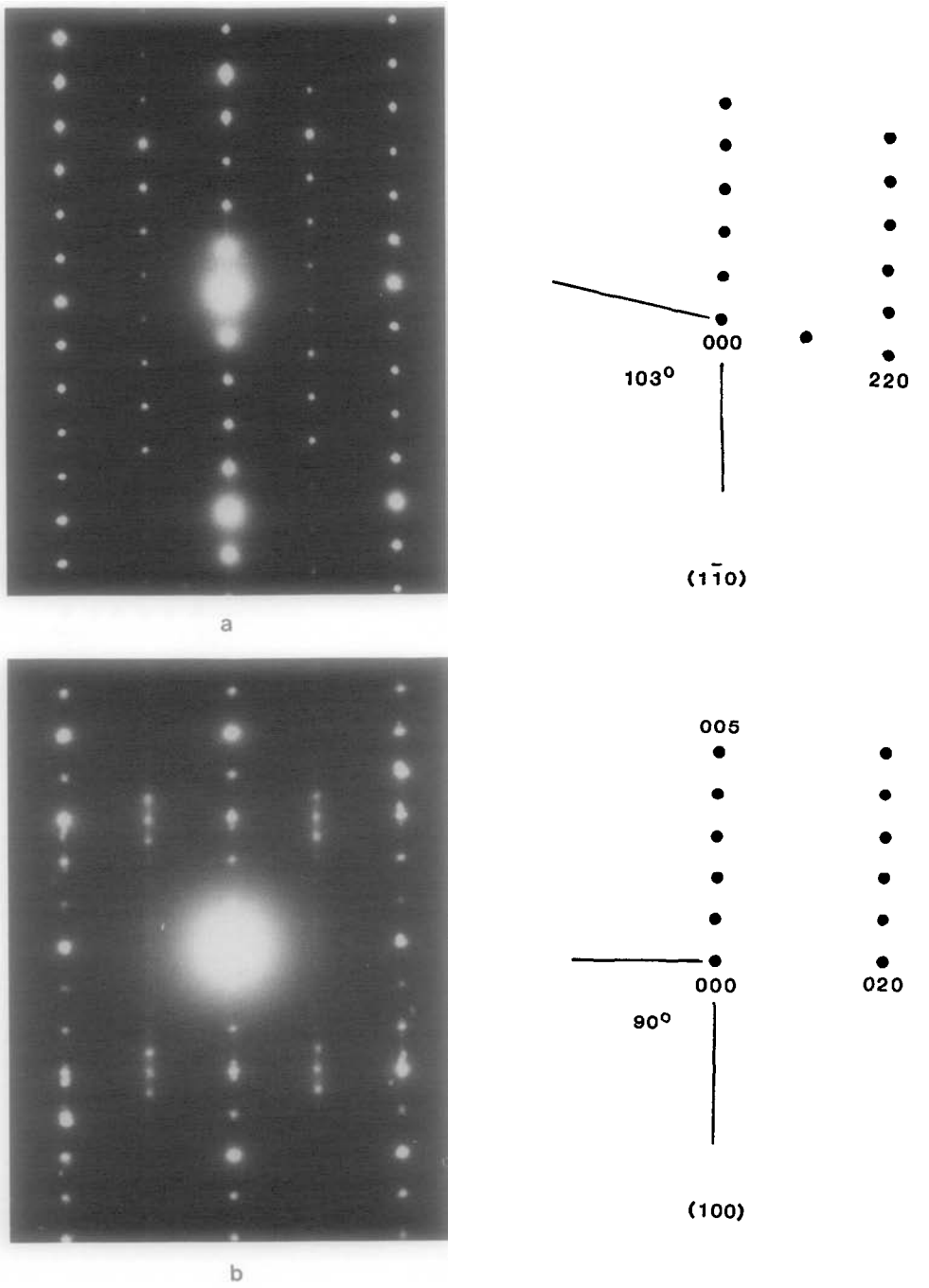

FIG. 8. (a) [110] and (b) [100] zone axis electron diffraction patterns of freshly prepared $Cs_2Ti_5O_{11}$. Note 5× periodicity of supercell with respect to subcell spot (005) and intense diffuse streaking midway between rows of sharp spots.

ably well for the [010] projection of orthorhombic $Cs_2Ti_6O_{13}$ ((*2*); a = 3.825 Å, b = 17.27 Å, c = 2.96 Å), but their instability in the electron beam suggests that they could be a hydrated form, such as the phase $Cs_{1.8}H_{0.8}Ti_6O_{13} \cdot 5H_2O$ reported in Ref. (*5*), which differs predominantly in the b parameter. The [001] patterns of the partially decomposed laths showed relatively intense streaking parallel to [100] through the subcell rows (Fig. 7c), indicating the presence of intergrowth defects. The corresponding [100] diffraction patterns did not show any new features.

Discussion

(*a*) *Identification of* $Cs_2Ti_5O_{11}$. The characteristic lath-like habit, together with the easily obtainable [001], [011], [100], and [110] reciprocal lattice sections, with associated superstructure scattering, provide useful electron-optical features for the positive identification of this phase. In synthetic SYNROC, or similar ceramic preparations, it may be necessary to detect quite small amounts, by volume fraction, in the total phase assemblage. It is therefore suggested that a portion of such specimens be dispersed on a holey carbon film and examined in a transmission electron microscope. The presence of even a few such needles, at magnifications of ca. 20,000×, will be readily apparent, since most of the other ceramics involved (hollandite, zirconolite, perovskite) form irregular wedge-shaped fragments on grinding.

If the ceramics have been subject to hydrothermal treatments, e.g., leaching tests, the presence of paracrystalline aggregates (cf. Fig. 2) in the image should be sought. Even electron diffraction patterns will not be helpful in this case and high-magnification images (>200,000×) will be required to characterize this material. The use of an analytical transmission electron microscope, capable of energy dispersive X-ray fluorescence analysis (cf. Ref. (*1*)) would allow positive identification of Cs. It should be noted that leach testing for Cs^{+1} uptake in water will quickly eliminate this phase from synthetic preparations. Thus small volume fractions could easily go into solution, undetected, without changing the long-term leaching characteristics, assuming the major Cs-containing phase was, for example, $(Cs,Ba)_x(Al,Ti)_8O_{16}$ or $Cs_xAl_xTi_{8-x}O_{16}$.

The use of ion-thinned or chemically thinned sections of the polycrystalline ceramic is not appropriate for the detection of small volume fractions of $Cs_2Ti_5O_{11}$, since it is likely to be preferentially etched from grain or phase boundaries.

(*b*) *Chemical stability of* $Cs_2Ti_5O_{11}$. The dehydrated phase is relatively inert under electron bombardment, but is apparently quite unstable chemically, at least in moist air, over extended periods of storage at room temperature. As reported in Ref. (*1*), freshly prepared $Cs_2Ti_5O_{11}$ may be seen to become wet, reacting with atmospheric water, if a small quantity is dispersed on filter paper. The crystals dissolve, leaving a wet patch which then dries leaving no apparent trace of the original crystals! If reasonable quantities are kept in sealed tubes, they can be kept for at least 2 years, apparently without change.

Conclusion

It should be clear from the above discussion that the presence of Cs-titanate phases, such as $Cs_2Ti_5O_{11}$ or $Cs_2Ti_5O_{11}(1 + x)H_2O$, or the related $Cs_2Ti_6O_{13} \cdot nH_2O$ series, are undesirable in SYNROC or other titanate ceramics designed for safe immobilization of radioactive ^{137}Cs.

Because of the fibrous habit, and sometimes indistinct nature of diffraction patterns of these phases, light optical mi-

croscopy and X-ray powder methods, or even electron probe chemical analysis using scanning mode techniques, may be insensitive to the presence of small volume fractions. Electron optical techniques, as described above, are essential for its detection.

Acknowledgments

The work in Melbourne was supported financially by the Australian Research Grants Committee, the Australian Institute for Nuclear Science and Engineering, and the University of Melbourne. J.K. is grateful for a University of Melbourne Post-Graduate Award. The high-resolution imaging in Cambridge was supported by the Science and Engineering Research Council (to D.J.S.).

References

1. L. A. BURSILL AND J. KWIATKOWSKA, *J. Solid State Chem.* **52,** 45 (1984).
2. I. E. GREY, I. MADSEN, J. WATTS, L. A. BURSILL, AND J. KWIATKOWSKA, *J. Solid State Chem.* **58,** 350 (1985).
3. T. WHITE, Reported at the 12th Australian Conference on Electron Microscopy, Brisbane (February 1984).
4. A. E. RINGWOOD, S. E. KESSON, N. G. WARE, W. O. HIBBERSON, AND A. MAJOR, *Geochem. J.* **13,** 141 (1979).
5. Y. FUJIKI, YU KOMATSU, T. SASAKI, AND N. OHTA, *J. Chem. Soc. Japan* **10,** 1656 (1981) (in Japanese; see also *Chem. Lett.* 1980, pp. 1023–1026).
6. J. KWIATKOWSKA, I. E. GREY, I. C. MADSEN, AND L. A. BURSILL, *J. Solid State Chem.* (1987), in press.
7. J. KWIATKOWSKA, Ph.D. thesis, University of Melbourne (1985).